Iterative, multiplexed CRISPR-mediated gene editing for functional analysis of complex protease gene clusters

Received for publication, June 21, 2019, and in revised form, August 19, 2019 Published, Papers in Press, September 9, 2019, DOI 10.1074/jbc.RA119.009773

LuLu K. Callies, Daniel Tadeo, Jan Simper, Thomas H. Bugge[1], and Roman Szabo

From the Proteases and Tissue Remodeling Section, NIDCR, National Institutes of Health, Bethesda, Maryland 20892

Edited by George N. DeMartino

Elucidation of gene function by reverse genetics in animal models frequently is complicated by the functional redundancy of homologous genes. This obstacle often is compounded by the tight clustering of homologous genes, which precludes the generation of multigene-deficient animals through standard interbreeding of single-deficient animals. Here, we describe an iterative, multiplexed CRISPR-based approach for simultaneous gene editing in the complex seven-member human airway trypsin-like protease/differentially expressed in a squamous cell carcinoma (HAT/DESC) cluster of membrane-anchored serine proteases. Through four cycles of targeting, we generated a library of 18 unique congenic mouse strains lacking combinations of HAT/DESC proteases, including a mouse strain deficient in all seven proteases. Using this library, we demonstrate that HAT/DESC proteases are dispensable for term development, postnatal health, and fertility and that the recently described function of the HAT-like 4 protease in epidermal barrier formation is unique among all HAT/DESC proteases. The study demonstrates the potential of iterative, multiplexed CRISPR-mediated gene editing for functional analysis of multigene clusters, and it provides a large array of new congenic mouse strains for the study of HAT/DESC proteases in physiological and in pathophysiological processes.

Functional redundancy is a long-recognized obstacle to the elucidation of gene function by the use of reverse genetics (1–6). Because of the frequent generation of homologous genes through gene duplication, this obstacle is frequently exacerbated by the genetic linkage of homologous genes, which often makes the generation of multigene-deficient animals through the standard interbreeding of animals with single gene deficiencies all but a practical impossibility. For example, in the genome of the mouse— one of the most frequently used model organisms for studying vertebrate gene function—within the family of proteolytic enzymes alone, there are more than 100 protease-encoding genes located within 10 gene clusters that range in size from 4 to 25 genes (Table S1).

The human airway trypsin-like protease/differentially expressed in squamous cell carcinoma (HAT/DESC)[2] subfamily of type II transmembrane serine proteases is an example of such a protease gene cluster (7–13). This cluster contains seven genes, (*Tmprss11a–g*), that encode proteases with high amino acid identity and largely overlapping patterns of expression, which predicts a high level of functional redundancy between individual family members (7, 14). Consistent with this notion, mice with individual deficiencies in the HAT/DESC proteases, TMPRSS11A and HAT, were reported to display no deleterious phenotype (14), whereas individual deficiency in a third HAT/DESC protease, HAT-like 4, results in only a nonlethal defect in epidermal barrier function (15).

Here we show that the simplicity and unsurpassed efficiency of CRISPR-mediated gene disruption (16) can be used for rapid analysis of multigene protease clusters through the generation of high-complexity "libraries" of congenic mouse strains with single and combined gene deficiencies. Specifically, we show that by using four iterative cycles of multiplexed CRISPR-mediated gene disruption, we were able to generate 18 unique mouse strains with single or multiple deficiencies in HAT/DESC proteases, including a mouse strain lacking all seven proteases. Furthermore, we used this library of mouse strains to show that the loss of all HAT/DESC proteases is compatible with normal development, postnatal survival, and reproduction and that the function of the HAT-like 4 protease in epidermal barrier formation is unique to HAT-like 4, with no contribution from any of the other six HAT/DESC proteases.

The described approach should prove useful for the functional analysis of other protease gene clusters, as well as for the analysis of gene clusters encoding other classes of homologous genes with predicted functional redundancy and close physical proximity. Furthermore, the large library of congenic, passenger mutation-free mouse strains generated in the study may prove valuable in elucidating the function of HAT/DESC proteases in normal physiology, as well as in pathological processes such as cancer, skin disorders, obstructive airway disease, and viral infection.

This work was supported by the NIDCR Intramural Research Program (to T. H. B). This work was also supported in part by NIDCR Gene Transfer Core Grant ZIC DE000744-04 and the NIDCR Veterinary Resources Core Grant ZIC DE000740-05. The authors declare that they have no conflicts of interest with the contents of this article. The content is solely the responsibility of the authors and does not necessarily represent the official views of the National Institutes of Health.

This article contains Tables S1–S3 and Fig. S1.

The data discussed in this publication have been deposited in NCBI's Gene Expression Omnibus and are accessible through GEO Series accession number GSE133070.

[1] To whom correspondence should be addressed: Proteases and Tissue Remodeling Section, NIDCR, National Institutes of Health, 30 Convent Dr., Rm. 3A-308, Bethesda, MD 20892. Tel.: 301-827-4804; Fax: 301-402-4804; E-mail: thomas.bugge@nih.gov.

[2] The abbreviation used is: HAT/DESC, human airway trypsin-like protease/differentially expressed in squamous cell carcinoma.

Table 1
The HAT/DESC subfamily of type II transmembrane serine proteases

Gene name	Protease name(s)	Human ortholog	NCBI reference sequence (mRNA; protein)
Tmprss11a	Transmembrane protease serine 11A, DESC-3, airway trypsin-like protease 1, esophageal cancer-susceptibility gene 1 protein	Yes	NM_001033233.2; NP_001028405.1
Tmprss11b	Transmembrane protease serine 11B, airway trypsin-like protease 5	Yes	NM_177024.4; NP_795998.2
Tmprss11c	Transmembrane protease serine 11C, neurobin, airway trypsin-like protease 3	No	NM_001030297.2; NP_001025468.1
Tmprss11d	Transmembrane protease serine 11D, adrenal secretory serine protease (AsP), human airway trypsin-like protease, MAT	Yes	NM_145561.2; NP_663536.1
Tmprss11e	Transmembrane protease serine 11E, DESC-1, transmembrane protease serine 11E2	Yes	NM_172880.2; NP_766468.1
Tmprss11f	Transmembrane protease serine 11F, airway trypsin-like protease 4	Yes	NM_178730.3; NP_848845.1
Tmprss11g	Transmembrane protease serine 11G, DESC-4, airway trypsin-like protease 2	No	NM_177162.4; NP_796136.2

Results

Construction of a large congenic library of HAT/DESC protease-deficient mice through iterative, multiplexed CRISPR-mediated gene editing

The human genome contains five *TMPRSS11* genes (*TMPRSS11A*, *TMPRSS11B*, *TMPRSS11D*, *TMPRSS11E*, and *TMPRSS11F*), all of which have orthologs in the mouse genome (*Tmprss11a*, *Tmprss11b*, *Tmprss11d*, *Tmprss11e*, and *Tmprss11f*). The mouse genome has two additional *Tmprss11* genes (*Tmprss11c* and *Tmprss11g*) for which no functional orthologs have been found in the human genome. A list of the seven *Tmprss11* genes with the commonly used name of the proteases they encode, as well as the NCBI reference sequences of their mRNA and protein is shown in Table 1. The seven mouse *Tmprss11* genes are located within a 0.5-Mb region of chromosome 5E1, syntenic with human chromosome 4q13.3, which harbors the five human *TMPRSS11* genes (7). All HAT/DESC proteases are type 2 transmembrane proteins that consist of a short N-terminal cytoplasmic tail, a signal anchor that forms a single-pass transmembrane domain, a SEA (sperm protein, enterokinase and agrin) domain, and a C-terminal serine protease domain (7).

To generate simultaneous null mutations in *Tmprss11* genes in the mouse germ line, we used CRISPRs designed to eliminate DNA sequences encoding all or part of the signal anchor to prevent insertion of the mutant protein into the endoplasmic reticulum membrane. We furthermore selected for mice carrying mutations introducing a shift in the reading frame to prevent the translation of any *Tmprss11* coding regions downstream from the deleted signal anchor. Founders were screened for CRISPR-induced mutations, and founders with desired mutations were tested for germ-line transmission through breeding to WT mice. For founders carrying mutations in more than one *Tmprss11* gene, the locations of these mutations on the same or opposite chromosomes were determined by the absence or presence of segregation of the mutant alleles within the F1 offspring. Established lines carrying desired mutant *Tmprss11* alleles in *cis* were then used as donors for successive rounds of CRISPR-mediated gene targeting, until a mouse line carrying mutations in all seven *Tmprss11* genes was generated. A list of the 18 congenic *Tmprss11* mutant mouse strains generated through this effort, including the specific mutation introduced into each *Tmprss11* gene, is shown in Table 2.

Because antibodies specific for each of the seven HAT/DESC proteases are not available and are unlikely to be successfully produced because of the high amino acid identity of these proteases, we asserted enhanced vigilance in assuring that the mutations introduced in each of the seven *Tmprss11* genes generated a null allele. First, we generated synthetic DNA corresponding to the predicted cDNA sequence of each of the seven WT and mutant *Tmprss11* alleles. These were inserted into an expression plasmid fused to a C-terminal c-Myc tag to allow for immunological detection of the recombinant proteins using mouse c-Myc antibodies. These plasmids then were transfected into HEK293T cells, and cell lysates from the transfected cells were analyzed by Western blotting. A protein exhibiting the expected molecular weight was detected in the cell lysate from cells transfected with plasmids expressing the WT cDNA (Fig. 1, *lanes 1*, *3*, *5*, *7*, *9*, *11*, and *13*). As expected, no protein product was detected in cell lysate or supernatant from cells transfected with plasmids expressing the mutant cDNAs (Fig. 1, *lanes 2*, *4*, *6*, *8*, *10*, *12*, and *14*). We also used RT-PCR of mRNA isolated from tongue and testes of mice bred to homozygosity for all seven mutant *Tmprss11* alleles (hereafter referred to as *Tmprss11a,b,c,d,e,f,g*$^{-/-}$) followed by DNA sequencing to search for alternatively spliced mRNAs for each of the mutant *Tmprss11* alleles that would restore an ORF and thereby be capable of producing truncated HAT/DESC protein products (albeit these would be unable to translocate to the extracellular/pericellular space or form disulfide bridges essential for protein folding and catalysis). However, no such mRNAs were identified (Fig. S1). Note that no *Tmprss11c* transcripts could be amplified, consistent with previous data (14). Taken together, these studies demonstrate that the CRISPR-mediated gene disruptions resulted in the introduction of combinations of null mutations into each of the seven *Tmprss11* genes. Furthermore, it demonstrates the feasibility of using iterative, multiplexed CRISPR-mediated gene editing for simultaneous targeting of multiple homologous genes.

Simultaneous loss of all HAT/DESC proteases is compatible with normal development and postnatal survival in mice

Tmprss11a,b,c,d,e,f,g$^{+/-}$ mice (with mutant alleles all located on the same chromosome; see Construction of a large congenic library of HAT/DESC protease-deficient mice through iterative, multiplexed CRISPR-mediated gene editing) were interbred to generate *Tmprss11a,b,c,d,e,f,g*$^{-/-}$ mice lacking all HAT/DESC proteases and WT littermates for comparison.

Table 2
Congenic *Tmprss11* knockout strains generated in this study

Strain name	Gene name	Mutation introduced	Protein product
T11.a	*Tmprss11a*	c.105_106insT	L36fsX48
T11.c	*Tmprss11c*	c.112_122delATCTTAACGGC	I38fsX65
T11.d	*Tmprss11d*	c.78delGinsTAGTAGGAGTTATAATAGCTA	V27fsX33
T11.e	*Tmprss11e*	c.54_58delGGTTA	W18fsX59
T11.f	*Tmprss11f*	c.122_126delTCGTA	I41fsX53
T11.g	*Tmprss11g*	c.58_76delGCCCTCATTACCGTGGCTC	A20fsX70
T11.cd	*Tmprss11c*	c.129_130insT	A44fsX69
	Tmprss11d	c.77delC	T26fsX28
T11.ge	*Tmprss11e*	c.55_56insG	V19fsX61
	Tmprss11g	c.52_55delACGG	T18fsX75
T11.ge-c[a]	*Tmprss11c*	c.115_119delTTAAC	L39fsX67
T11.ge-d[a]	*Tmprss11d*	c.68_84delTCATAATAACGGTAGGG	V23fsX38
T11.ge-f[a]	*Tmprss11f*	c.45_46insTCTCTCCAAATGGGCAAAGGATGTGAAGATATTTGTGTCCCATGTAAA TGCTCACCAAAAGGTGACTTCAGCCGAGGAGGAGTTCAATAATCAAGTGGATAAGA TGACCCGTTCTGTGGACAGTCAGCCTCTCTCCCCAGCCATCCCTGTCATTGCTCAA TGGGCACATGAACAAAGTGGTCATGGTGGTCGAGATGGAGGTTATGCTTGGGCTCA GCAACACGGGCTTCCACTCACCAAAGCTGACCTGGCTACTGCTGAGGTAG	I16fsX45
T11.ge-cd[a]	*Tmprss11c*	c.129_130insTT	A44fsX48
	Tmprss11d	c.77_81delCGGTAinsG	T26fsXfsX31
T11.ge-cd-a[b]	*Tmprss11a*	c.97-102delATTGGAinsTCCTTCCAAGGTAAAAGGCTTAAAGTCCACGGCCTGT	I33fsX57
T11.ge-cd-b[b]	*Tmprss11b*	c.26-38delGCAAATCTATCCC	R9fxX11
T11.ge-cd-f[b]	*Tmprss11f*	c.48_52delCGAAT	E17fsX53
T11.ge-cd-ab[b]	*Tmprss11a*	c.101delG	34GfsX58
	Tmprss11b	c.25_26delTC	V5fsX52
T11.ge-cd-af[b]	*Tmprss11a*	c.96_103delCATTGGAC	I33fsX44
	Tmprss11f	c.48_52delCGAAT	E17fsX53
T11.all[c]	*Tmprss11f*	c.122_124delTCGinsGAGCACATGGGCACATGAACAAAGTGGCCATGGTGGTCGA GATGGAGGTTATGCTTGGGCTCAGCAACATGGGCTTCCACTCACCAAGGCTGACCT GGCTACAGCTGCTGCTGATTGCCAGATCTGCCAACAGCAGAAACCAACACTGAGCC CCAGATATGGCACCATTCCTCGAGGTGACCAGCCAGCAACCTGGTGGCAGGTTGAC TACATTGGACCACTTCCTTCGTGGAAAGGACAGCGTTTTGTTCTTACTGGAGTAGA TACTTATTCTGGTTATGGATTTGCCTTTCCTGCACGTAATGCCTCTGCTAAAACCA CCATTCACGGACTGACAGAATGCCTCATCTATCGTCATGGTATTCCACACAGTATT GCTTCTGACCAAGGAACTCATTTCACAT	I41fsX90

[a] Contains all mutations present in T11.ge.
[b] Contains all mutations present in T11.ge-cd.
[c] Contains all mutations present in T11.ge-cd-ab.

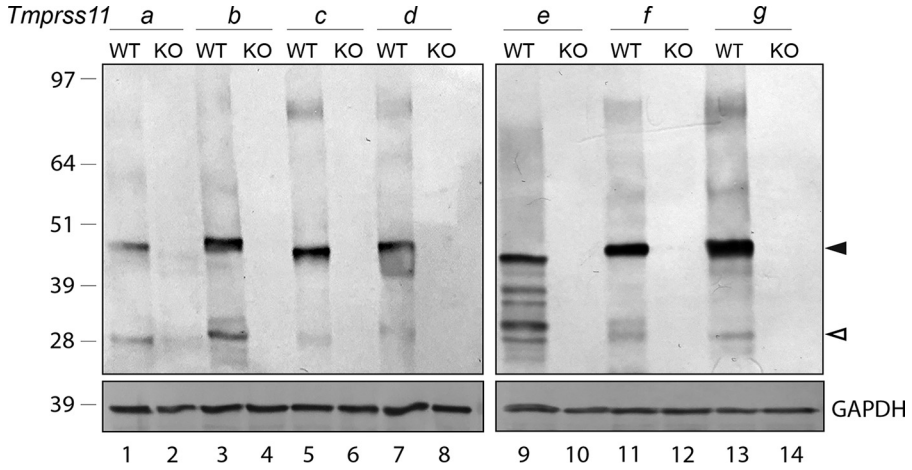

Figure 1. Generation of null mutations in the seven mouse *Tmprss11* genes. *Upper panels*, synthetic DNA corresponding to the predicted cDNA sequence of each of the seven WT and mutant *Tmprss11* alleles were inserted into an expression plasmid fused to a C-terminal c-Myc tag. The plasmids were transfected into HEK293T cells, and cell lysates from the transfected cells were analyzed 2 days after transfection by reducing SDS/PAGE followed by Western blotting using mouse anti–c-Myc antibodies. Positions of molecular mass markers (kDa) are shown on the *left*. Positions of putative full-length (*filled arrowhead*) and putative activation site-cleaved (*open arrowhead*) proteases are shown on the *right*. *Lower panels*, a separate Western blotting of the same protein samples probed with glyceraldehyde-3-phosphate dehydrogenase (*GAPDH*) antibodies.

Surprisingly, genotyping of offspring from these crosses at birth (Fig. 2*A*) or at weaning (Fig. 2*B*) showed a Mendelian inheritance of the *Tmprss11a,b,c,d,e,f,g*$^{-}$ allele, demonstrating that the simultaneous loss of all HAT/DESC proteases is compatible with both embryonic and postnatal development. To study the impact of loss of all HAT/DESC proteases on long-term health and survival, we next set up separate cohorts of female and male *Tmprss11a,b,c,d,e,f,g*$^{-/-}$ mice and their associated *Tmprss11a,b,c,d,e,f,g*$^{+/-}$ and WT littermates. The health and survival of mice in these cohorts were prospectively monitored by weekly outward inspection and weight measurement. Interestingly, neither female nor male *Tmprss11a,b,c,d,e,f,g*$^{-/-}$ mice that could be followed for at least 6 months after weaning displayed obviously abnormal appearance, abnormal weight gain or weight loss (Fig. 2, *C* and *D*), or increased mortality (Fig. 2, *E* and *F*).

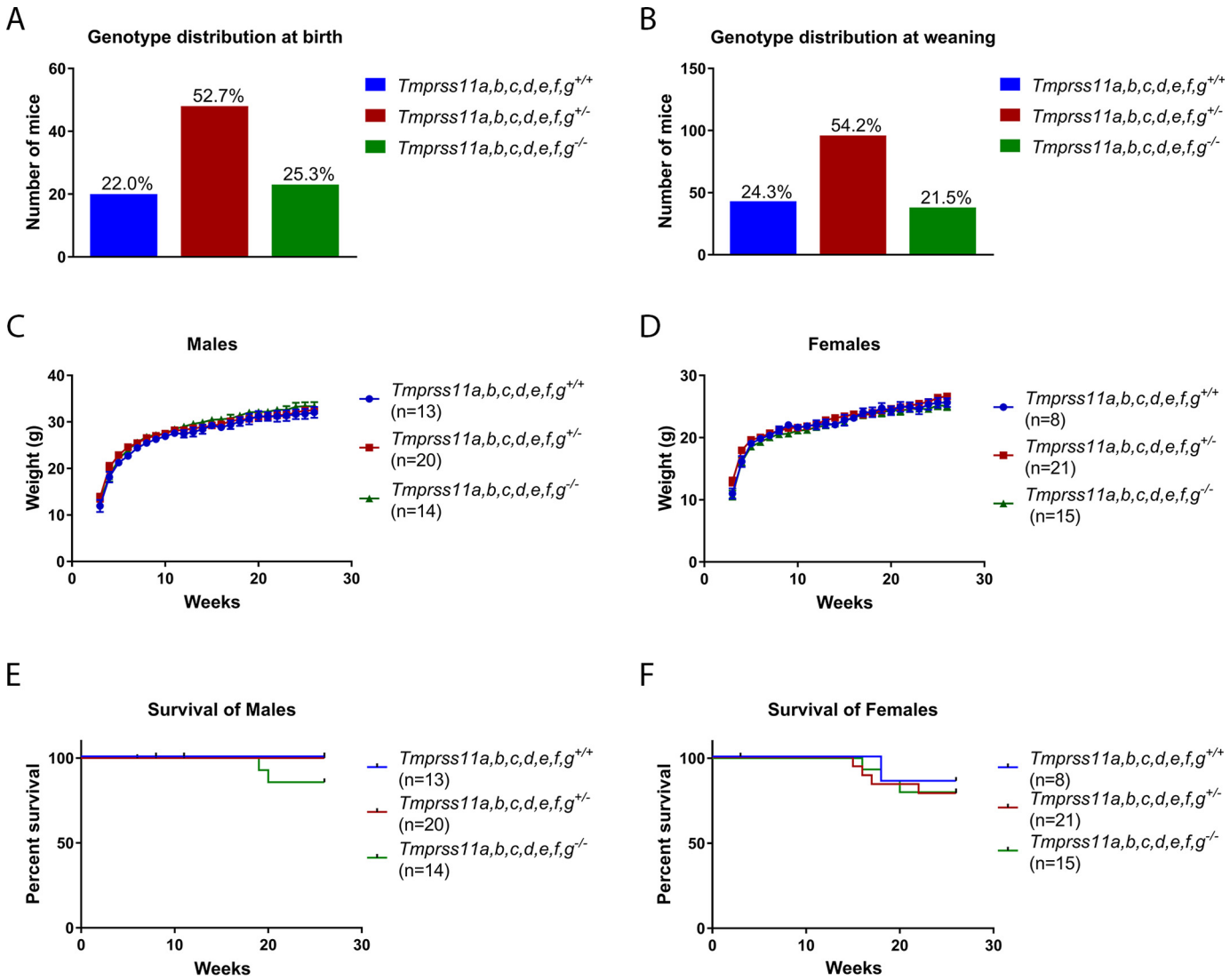

Figure 2. Simultaneous loss of all HAT/DESC proteases is compatible with mouse development and postnatal survival. *A* and *B*, genotype distribution of 94 offspring at birth (*A*) and of 166 offspring at weaning (*B*) from intercrossed *Tmprss11a,b,c,d,e,f,g*$^{+/-}$ mice. *C* and *D*, body weights of male (*C*) and female (*D*) *Tmprss11a,b,c,d,e,f,g*$^{+/+}$ (*blue circles*), *Tmprss11a,b,c,d,e,f,g*$^{+/-}$ (*red squares*), and *Tmprss11a,b,c,d,e,f,g*$^{-/-}$ (*green triangles*) mice followed for up to 26 weeks after birth. The *numbers* in *parentheses* indicate the number of mice initially enrolled in the cohort. The data are shown as means ± S.E. *E* and *F*, Kaplan–Meier plots of the survival of male (*E*) and female (*F*) *Tmprss11a,b,c,d,e,f,g*$^{+/+}$ (*blue lines*), *Tmprss11a,b,c,d,e,f,g*$^{+/-}$ (*red lines*), and *Tmprss11a,b,c,d,e,f,g*$^{-/-}$ (*green lines*) mice followed from weaning and up to 26 weeks after birth. The *numbers* in *parentheses* indicate the number of mice initially enrolled in the cohort.

We next collected organs from *Tmprss11a,b,c,d,e,f,g*$^{-/-}$ mice and WT littermates and prepared hematoxylin and eosin-stained sections for histological analysis (Fig. 3). Consistent with their normal development, weight gain, normal outward appearance, and survival, no histological abnormalities were observed in skin, tongue, colon, small intestine, testis/uterus, liver, kidney, lungs, or trachea of *Tmprss11a,b,c,d,e,f,g*$^{-/-}$ mice when compared with their WT littermates.

Fertility of mice lacking all HAT/DESC proteases

Several *Tmprss11* genes are co-expressed in reproductive organs, including uterus and testis (14), suggesting possible unique or shared functions of HAT/DESC proteases in reproduction. To test this, we examined the litter frequency (Fig. 4*A*) and litter size (Fig. 4*B*) of intercrossed *Tmprss11a,b,c,d,e,f,g*$^{-/-}$ mice as compared with intercrossed *Tmprss11a,b,c,d,e,f,g*$^{+/-}$ mice. This analysis showed no indication of impaired fertility in mice lacking all HAT/DESC proteases when compared with their HAT/DESC–sufficient littermates.

Mice lacking all HAT/DESC proteases display impaired epidermal barrier function, which is solely attributable to the loss of HAT-like 4

Mice with a single deficiency in *Tmprss11f*, encoding HAT-like 4, were recently reported to display a defect in epidermal barrier function, which manifests at birth and persists throughout adulthood (15). This would predict that *Tmprss11a,b,c,d,e,f,g*$^{-/-}$ mice, which in addition to lacking HAT-like 4, are deficient in all other epidermally expressed HAT/DESC proteases, would display a similar or more pronounced loss of epidermal barrier function. Indeed, transepidermal water loss was significantly increased in newborn *Tmprss11a,b,c,d,e,f,g*$^{-/-}$ mice when compared with their *Tmprss11a,b,c,d,e,f,g*$^{+/-}$ and WT littermates (Fig. 5*A*). Fur-

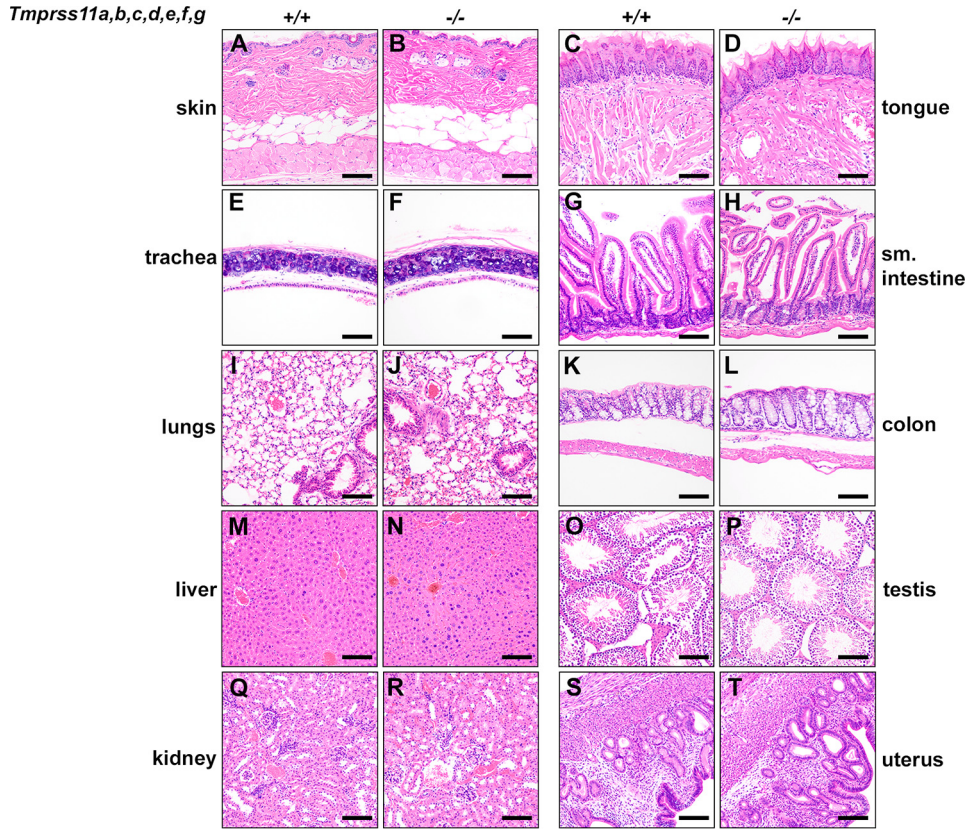

Figure 3. Histological appearance of tissues of mice lacking all HAT/DESC proteases. H&E-stained sections of skin (*A* and *B*), tongue (*C* and *D*), trachea (*E* and *F*), small (*sm.*) intestine (*G* and *H*), lung (*I* and *J*), colon (*K* and *L*), liver (*M* and *N*), testis (*O* and *P*), kidney (*Q* and *R*), and uterus (*S* and *T*) of 6-month-old *Tmprss11a,b,c,d,e,f,g*$^{+/+}$ mice (*A*, *C*, *E*, *G*, *I*, *K*, *M*, *O*, *Q*, *S*) and *Tmprss11a,b,c,d,e,f,g*$^{-/-}$ littermates (*B*, *D*, *F*, *H*, *J*, *L*, *N*, *P*, *R*, *T*). *Scale bar* is 100 μm.

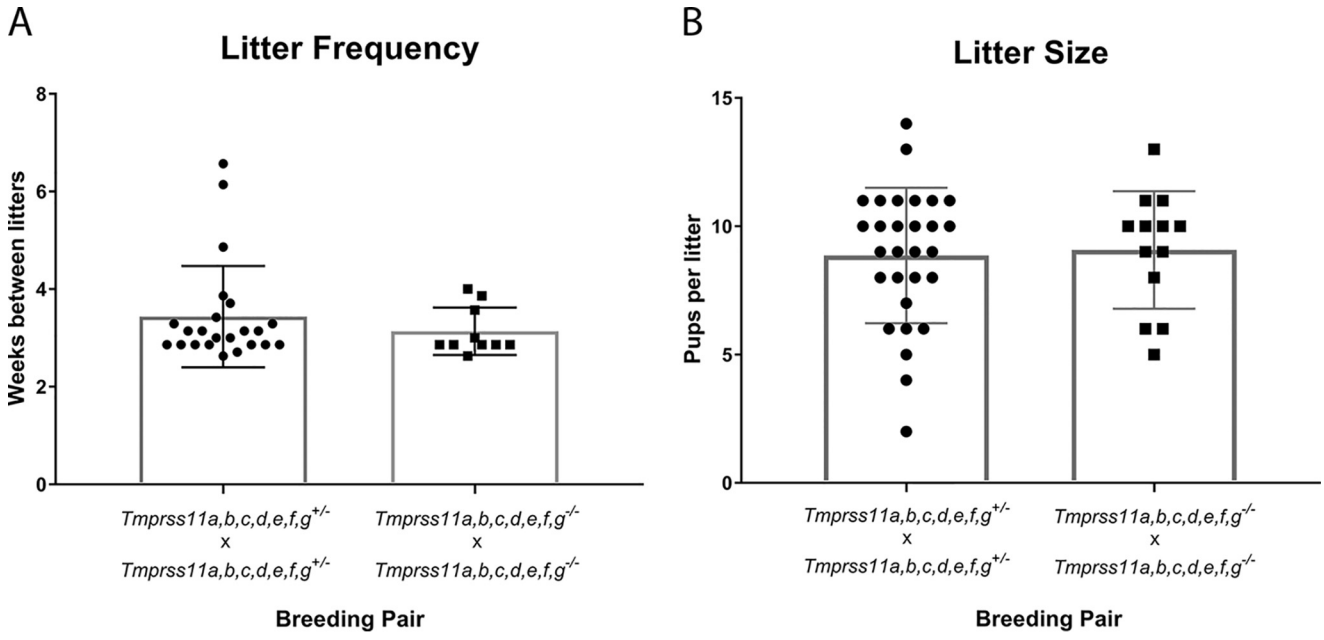

Figure 4. Loss of all HAT/DESC proteases is compatible with female and male fertility. *A* and *B*, frequency of litters (*A*) and size of litters (*B*) of intercrossed *Tmprss11a,b,c,d,e,f,g*$^{-/-}$ mice (*squares*, three breeding pairs analyzed) and intercrossed *Tmprss11a,b,c,d,e,f,g*$^{+/-}$ littermates (*circles*, seven breeding pairs analyzed). The data are shown as individual values with means ± standard deviation of the mean.

thermore, in mice with a single deficiency in *Tmprss11f* (generated in this study; Table 2), an increase in transepidermal water loss very similar to the published rate of water loss (15) was observed (Fig. 5*B*). Among the 18 congenic mouse strains generated in this study were mice that are deficient in all HAT/DESC proteases, except HAT-like 4 (*Tmprss11a,b,c,d,e,g*$^{-/-}$ mice; Table 2), providing an opportunity to query the role of each of these genes in epidermal barrier function. Surprisingly,

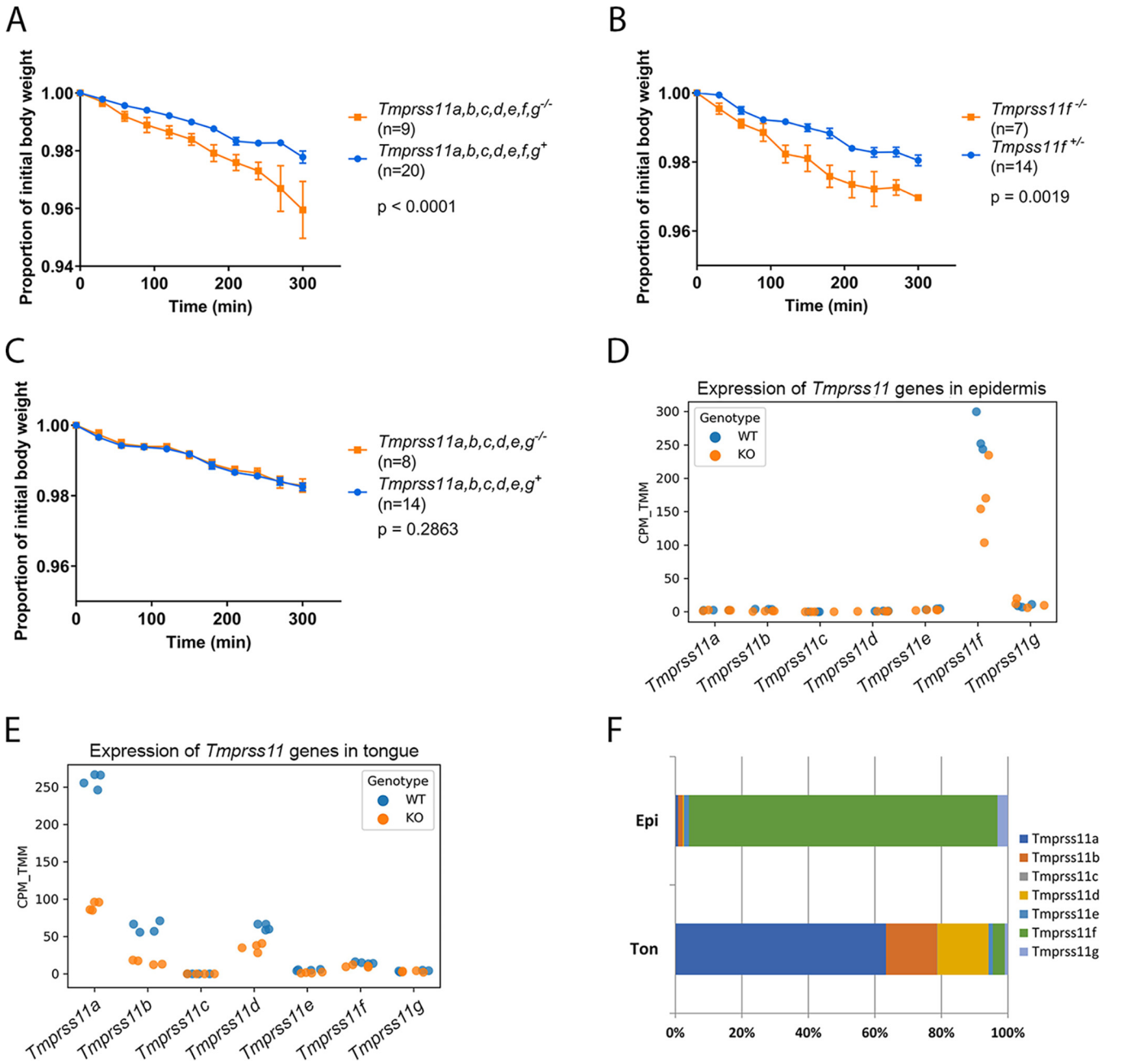

Figure 5. Impaired barrier function of mice lacking all HAT/DESC proteases is solely due to loss of HAT-like 4. *A–C*, transepidermal water loss was measured over a 300-min period in newborn *Tmprss11a,b,c,d,e,f,g*$^{-/-}$ mice (*A*, *orange squares*) and their *Tmprss11a,b,c,d,e,f,g*$^{+/-}$ and *Tmprss11a,b,c,d,e,f*$^{+/+}$ littermates (*A*, *blue circles*, shown as one group), newborn *Tmprss11f*$^{-/-}$ mice (*B*, *orange squares*) and their *Tmprss11f*$^{+/-}$ littermates (*B*, *blue circles*), and newborn *Tmprss11a,b,c,d,e,g*$^{-/-}$ mice (*C*, *orange squares*) and their *Tmprss11a,b,c,d,e,g*$^{+/-}$ and *Tmprss11a,b,c,d,e,g*$^{+/+}$ littermates (*C*, *blue circles*, shown as one group). The *numbers* in *parentheses* indicate the number of mice per group. The data are shown as means ± S.E. The *p* values were determined by linear regression analysis (two-tailed) using GraphPad Prism software. *D* and *E*, expression levels of mRNAs of the seven *Tmprss11* genes in the epidermis (*D*) and in the tongue (*E*) of *Tmprss11a,b,c,d,e,f,g*$^{+/+}$ mice (*blue circles*) and their *Tmprss11a,b,c,d,e,f,g*$^{-/-}$ littermates (*orange circles*). The data are shown as individual values of each mouse and are expressed as number of reads per million reads after trimmed mean of *M* value normalization (*CPP_TMM*). *F*, relative expression level of each of the seven *Tmprss11* genes in epidermis (*top*, *Epi*) and tongue (*bottom*, *Ton*) of *Tmprss11a,b,c,d,e,f,g*$^{+/+}$ mice shown as the percentage of total *Tmprss11* transcripts in the two tissues.

transepidermal water loss in *Tmprss11a,b,c,d,e,g*$^{-/-}$ mice was identical to their *Tmprss11a,b,c,d,e,g*$^{+/-}$ and WT littermates (Fig. 5*C*), revealing that HAT-like 4 is solely responsible among HAT/DESC proteases for maintaining epidermal barrier function with no compensation by any of the six other HAT/DESC proteases. Six *Tmprss11* genes (14) have been shown to be expressed in mouse skin (*Tmprss11a*, *Tmprss11b*, *Tmprss11d*, *Tmprss11e*, *Tmprss11f*, and *Tmprss11g*), making the failure of any of the other five *Tmprss11* genes to compensate for the loss of *Tmprss11f* somewhat unexpected. To further investigate this, we performed an RNAseq analysis of skin from newborn mice to obtain quantitative estimates of the level of expression of each of the six *Tmprss11* genes (Fig. 5, *D* and *F*). Tongue, an organ also rich in keratinized tissue and expressing the same six *Tmprss11* genes (14), was included in the analysis for comparison. This analysis confirmed that *Tmprss11a*, *Tmprss11b*,

Tmprss11d, *Tmprss11e*, *Tmprss11f*, and *Tmprss11g* were expressed in the two organs (Fig. 5, *D–F*; GEO accession number GSE133070). Interestingly, however, in the skin, more than 90% of all *Tmprss11* transcripts were derived from the *Tmprss11f* gene. This expression pattern was strikingly different in the tongue, where three *Tmprss11* genes (*Tmprss11a*, *Tmprss11b*, and *Tmprss11d*) were all prominently expressed. This indicates that the lack of functional compensation for the loss of *Tmprss11f* by other *Tmprss11* genes as regards epidermal barrier function is likely due to the preponderant expression of *Tmprss11f* in skin rather than to a unique functional property of the HAT-like 4 protease.

Absence of compensatory gene expression in mice lacking all HAT/DESC proteases

The lack of robust developmental or postnatal phenotypes in animals in response to targeted gene disruptions is often attributed to compensatory changes in gene expression. We therefore next performed a global transcriptomic analysis by comparing gene expression levels in skin and tongue of newborn *Tmprss11a,b,c,d,e,f,g*$^{-/-}$ mice and their WT littermates by RNAseq analysis. The complete data set was deposited in the GEO database (accession number GSE133070). A total of 23,420 genes were compared, and gene expression differences were analyzed. Surprisingly, no genes were found to be significantly up- or down-regulated in response to the simultaneous loss of all *Tmprss11* genes using an adjusted p value of <0.05. Furthermore, no trend was observed toward enhanced or decreased expression of genes encoding other membrane-anchored serine proteases (*St14*, *Prss8*, and *Tmprss13*) or membrane-anchored serine protease inhibitors (*Spint1* and *Spint2*) with known importance for epidermal barrier function (17–22). Likewise, mRNAs for desquamation-associated kallikreins (*Klk5*, *Klk7*, and *Klk14*) and their principal inhibitor (*Spink5*) were expressed at similar levels in *Tmprss11a,b,c,d,e,f,g*$^{-/-}$ mice and WT littermates.

Discussion

Functional redundancies of homologous genes, compounded by their frequent genetic linkage, remain serious impediments to the use of reverse genetics to elucidate physiological and pathophysiological gene functions in model organisms. This includes the functional study of the more than 600 genes in the mouse genome that encode proteolytic enzymes (23). Here, we describe the application of an iterative, CRISPR-based approach for multiplexed gene disruption and its use for functional analysis of the seven-member gene cluster encoding the mouse HAT/DESC subfamily of type II transmembrane serine proteases (7–13). By using an iterative approach, through four cycles of targeting, we were able to generate a total of 18 unique congenic mouse strains with single or multiple gene deficiencies, including a mouse strain that lacked all seven HAT/DESC proteases. The described approach should be readily amenable to functional studies of other protease gene clusters and to the functional study of homologous, genetically linked genes in general.

HAT/DESC proteases have mainly been studied as modulators of human diseases that afflict the skin, airways, and upper digestive tract, which represent main sites of their expression. In the context of cancer, individual HAT/DESC proteases (DESC1, HAT, and HAT-like 5) have been identified as either promotors of human tumorigenesis (24–26) or as putative tumor suppressors (DESC1, HAT, HAT-like 5, and TMPRSS11A) (27–30). HAT has been proposed to promote chronic airway disease through its ability to induce inflammatory cytokine and mucin production (31, 32) but also to ameliorate bleomycin-induced pulmonary fibrosis by suppressing several pro-inflammatory pathways (33). Additionally, HAT was reported to exacerbate psoriasis vulgaris symptoms via induction of cytokine release (34).

As of yet, few validated substrates for HAT/DESC proteases have been reported. Like many membrane-anchored serine proteases (35), HAT can activate protease-activated receptor-2 in cell-based assays (36) and can cleave macrophage-stimulating protein (37), fibrinogen (38), and the urokinase plasminogen activator receptor (39). Most recently, HAT like-5 was reported to cleave basigin, a chaperone of the lactate monocarboxylate transporter, MCT4, to promote lung cancer progression (25). Interestingly, DESC1, HAT, and TMPRSS11A also have emerged as essential processing proteases for maturation of envelope glycoproteins of highly pathogenic viruses, including several influenza A viruses and severe acute respiratory syndrome coronavirus (40–48).

Because of the relative paucity of knowledge regarding the physiological functions of HAT/DESC proteases, in this study, we undertook a systematic genetic analysis of these proteases in mice. Because the high amino acid identity and substantial overlap in tissue expression of HAT/DESC proteases predicted a considerable level of functional redundancy, we hypothesized that a robust phenotype might only manifest after simultaneous removal of several HAT/DESC proteases. Remarkably, however, even mice having all seven *Tmprss11* genes inactivated displayed no overt developmental or postnatal phenotype, when assayed for Mendelian inheritance, pre- and post-weaning survival, outward health, weight gain, fertility, and histological appearance of major organs. Furthermore, mice lacking all HAT/DESC proteases showed no trend toward compensatory gene expression in whole-transcriptome analysis of two tissues with high *Tmprss11* gene expression. Mice carrying mutations in all *Tmprss11* genes, however, did display a defect in epidermal barrier function, as was recently described for mice with a single deficiency in *Tmprss11f* (15). Contrary to our prediction of functional redundancy between HAT/DESC proteases, however, by using the library of *Tmprss11* mutants generated in this study, we were able to unequivocally demonstrate that the barrier defect in mice lacking all *Tmprss11* genes is solely attributable to the loss of *Tmprss11f*. This was evident by the comparative transepidermal water loss rates in mice lacking all *Tmprss11* genes and mice lacking only *Tmprss11f* and, more importantly, by the absence of a barrier defect in mice lacking all *Tmprss11* genes, except *Tmprss11f*.

In summary, we have demonstrated the feasibility of using iterative, multiplexed CRISPR-mediated gene targeting to construct large libraries of congenic, passenger mutation-free mouse strains for the functional analysis of multigene clusters. Furthermore, we believe that the 18 mouse strains generated in

this study will prove to be a valuable community resource facilitating the elucidation of the physiological functions of HAT/DESC proteases, as well as determining the contribution of this relatively unexplored protease subfamily to cancer, inflammatory diseases, fibrosis, viral infection, and other diseases.

Experimental procedures

Animal work

All experiments involving mice were performed in an Association for Assessment and Accreditation of Laboratory Animal Care International–accredited vivarium following Institutional Guidelines and Standard Operating Procedures as approved by the NIDCR Institutional Animal Care and Use Committee.

Generation of Tmprss11-deficient mouse strains

Two guide RNAs that target the signal anchor domain–encoding exons of each of the seven mouse *Tmprss11* genes (Table S2) were designed by using the CRISPR guide RNA design tool developed by Dr. Feng Zhang's lab at MIT (49). All 14 guide RNAs were cloned into the SpCas9 and chimeric guide RNA expression plasmid pX330 (Addgene catalog no. 42230) (50). Successful cloning of each of the guides was confirmed by DNA sequencing. To generate the *Tmprss11*-targeted mouse strains, plasmids containing guide RNA were mixed equimolarly and diluted to a final concentration of 5–10 ng/μl in 10 mM Tris/HCl, pH 7.4, 0.1 mM EDTA. The pDNA mix was then microinjected into the male pronucleus of FVB/NJ zygotes, which were implanted into pseudopregnant mice. All founders were screened for any changes in the targeted regions of any of the seven *Tmprss11* genes by PCR amplification followed by DNA sequencing (Table S3 for sequences of PCR primers used for founder screening). Mice carrying gene-inactivating mutations were bred to FVB/NJ WT mice to test the germ-line transmission and, in case of multiple mutations present in a single founder, for genetic linkage. Four rounds of CRISPR/Cas9-mediated targeting was used to generate a strain carrying mutations in all seven *Tmprss11* genes and 17 mouse strains with mutations in one or more *Tmprss11* gene (see "Results" and Table 2 for details). Depending on the strain, offspring were genotyped by PCR using either primers used in the original screening or designed to specifically detect knockout and WT alleles of the targeted gene or genes, followed by DNA sequencing when necessary (Table S3).

Cell culture and transfection

HEK293T cells were grown in 6-well plates in high glucose Dulbecco's modified Eagle's medium (Gibco) containing penicillin, streptomycin and 10% fetal bovine serum until reaching 90% confluence. pCMV6-AC-Myc expression plasmids (catalog no. PS100003; OriGene Technologies, Rockville, MD) carrying C-terminal Myc-tagged WT and mutant variants of mouse *Tmprss11* cDNA were synthesized by Blue Heron Biotech (Seattle, WA). 2500 ng of plasmid was transfected into cells using Lipofectamine 3000 reagent (Invitrogen) according to the manufacturer's protocol. Transfected cells were grown in serum-free, high-glucose Dulbecco's modified Eagle's medium.

Western blotting

Two days after transfection, the cells were lysed in 2% SDS, 10% glycerol, and 6.25 mM Tris/HCl, pH 6.8. 100 μg of each sample was deglycosylated with an enzymatic protein deglycosylation kit (Thermo Fisher) according to the manufacturer's protocol. For Western blotting analysis, 40 μg of each deglycosylated sample was reduced in NuPAGE sample buffer (Thermo Fisher) containing 7% β-mercaptoethanol by boiling for 5 min. The samples were loaded into a 4–12% Bis-Tris gel (Thermo Fisher) and run in NuPAGE MOPS running buffer (Thermo Fisher) at 150 V for 90 min. Samples were transferred to a polyvinylidene difluoride membrane (0.2-μm pore size; Thermo Fisher) in NuPAGE transfer buffer (Thermo Fisher) for 1 h at 30 V. The membrane was blocked for 30 min using TBST (Fisher Scientific) containing 0.05% Tween 20 (Sigma–Aldrich) with 5% dry milk. To detect protein, the membrane was incubated overnight at 4 °C with 1 μg/μl mouse anti–c-Myc primary antibody (9B11; Cell Signaling Technology, Danvers, MA). Subsequently, three 5-min washes with TBST were performed before incubating the membrane for 1 h with 1 μg/μl goat anti-mouse secondary antibody conjugated with alkaline phosphatase (D0487; Agilent, Santa Clara, CA). After incubation, three 5-min washes with TBST were performed before developing the membrane in nitro blue tetrazolium chloride and 5-bromo-4-chloro-3′-indolyphosphate *p*-toluidine salt (Thermo Fisher). Development was stopped by washing the membrane in water.

cDNA sequencing

Tongue and testis were collected from *Tmprss11a,b,c,d,e,f,g*$^{-/-}$ mice and their WT littermates aged 6–7 weeks. RNA was isolated from tissues using TRIzol reagent (Thermo Fisher) according to the manufacturer's protocol. cDNA was synthesized using 1000 ng of RNA, using the RevertAid H minus cDNA synthesis kit (Thermo Fisher) and sequenced. The PCRs included denaturation at 95 °C followed by 40 cycles with 1 min of denaturation at 95 °C, 1 min of annealing at 55 °C, and 2 min of elongation at 72 °C before a final extension at 72 °C for 5 min. Sequencing data were compared with expected sequences for *Tmprss11* WT genes and were examined for alternative splice variants that could produce protein products.

Transepidermal fluid loss

Fluid loss in newborn mice was measured as a percentage of decrease in body weight, with measurements taken every 30 min for 5 h.

RNAseq and analysis

Skin and tongue were collected from newborn mice. Tissues were frozen on dry ice and stored at −80 °C before further processing. Epidermis was manually separated from dermis after incubation for 5 min at 60 °C in 5 mM EDTA. Tissues were homogenized in TRIzol reagent, and RNA was extracted according to the manufacturer's protocol (Thermo Fisher). Double-stranded cDNA was prepared using the SMARTer V4 ultra-low input kit (Clontech). Libraries were prepared using a TruSeq v2 kit (Illumina, San Diego, CA), individually barcoded,

pooled to a 2 nM final concentration, and sequenced on a NextSeq500 sequencer (Illumina) using 37 × 37 paired-end mode. The base-called demultiplexed (fastq) read qualities were determined using FastQC (v0.11.2) (http://www.bioinformatics.babraham.ac.uk/projects/fastqc/),[3] aligned to the GENCODE M11 mouse genome (GRCm38.p4), and gene counts were generated using STAR (v2.5.2a) (51). Post-alignment qualities were generated with QoRTS (version 1.1.6) (52). An expression matrix of raw gene counts was generated using R and filtered to remove low counts genes (defined as those with fewer than five reads in all samples). The filtered expression matrix was used to generate a list of differentially expressed genes between the sample groups using DESeq2 (53).

Assessment of long-term health

Littermate *Tmprss11a,b,c,d,e,f,g*$^{-/-}$, *Tmprss11a,b,c,d,e,f,g*$^{+/-}$, and WT mice were kept in HEPA-filtered, mixed genotype cages of up to five mice. The mice were weighed weekly, and outward health was assessed. The mice were euthanized after 6 months, and organs (dorsal skin, tongue, colon, small intestine, liver, kidney, uterus/testis, trachea, and lungs) were collected. Organs were fixed overnight in Z-fix (Anatech LTD), paraffin-embedded, sectioned, and hematoxylin- and eosin-stained. Examination of tissues was performed by light microscopy.

Analysis of fertility

Breeding pairs of female and male *Tmprss11a,b,c,d,e,f,g*$^{-/-}$ mice and their female and male *Tmprss11a,b,c,d,e,f,g*$^{+/-}$ littermates were established after weaning and genotyping. The breeding pairs were observed daily, and if pups were found, litter size and date of birth were recorded. Fertility was measured in terms of litter size and frequency. Litter frequency was calculated as the average number of weeks between litters for each breeder pair.

Author contributions—L. K. C., T. H. B., and R. S. formal analysis; L. K. C., D. T., J. S., T. H. B., and R. S. investigation; L. K. C., T. H. B., and R. S. writing-original draft; L. K. C., D. T., J. S., T. H. B., and R. S. writing-review and editing; T. H. B. and R. S. conceptualization; T. H. B. and R. S. supervision; T. H. B. funding acquisition; R. S. methodology.

Acknowledgments—We thank Dr. Mary Jo Danton for critically reviewing this manuscript, and Andrew Cho from the NIDCR Gene Transfer Core for transgenic mouse generation.

References

1. Rudnicki, M. A., and Jaenisch, R. (1995) The MyoD family of transcription factors and skeletal myogenesis. *Bioessays* **17,** 203–209 CrossRef Medline
2. Luo, J., Pasceri, P., Conlon, R. A., Rossant, J., and Giguère, V. (1995) Mice lacking all isoforms of retinoic acid receptor beta develop normally and are susceptible to the teratogenic effects of retinoic acid. *Mech. Dev.* **53,** 61–71 CrossRef Medline
3. Bentley, D., Selfridge, J., Millar, J. K., Samuel, K., Hole, N., Ansell, J. D., and Melton, D. W. (1996) DNA ligase I is required for fetal liver erythropoiesis but is not essential for mammalian cell viability. *Nat. Genet.* **13,** 489–491 CrossRef Medline
4. St-Jacques, B., and McMahon, A. P. (1996) Early mouse development: lessons from gene targeting. *Curr. Opin. Genet. Dev.* **6,** 439–444 CrossRef Medline
5. Melton, D. W. (1994) Gene targeting in the mouse. *Bioessays* **16,** 633–638 CrossRef Medline
6. Shastry, B. S. (1994) More to learn from gene knockouts. *Mol. Cell. Biochem.* **136,** 171–182 CrossRef Medline
7. Hobson, J. P., Netzel-Arnett, S., Szabo, R., Rèhault, S. M., Church, F. C., Strickland, D. K., Lawrence, D. A., Antalis, T. M., and Bugge, T. H. (2004) Mouse DESC1 is located within a cluster of seven DESC1-like genes and encodes a type II transmembrane serine protease that forms serpin inhibitory complexes. *J. Biol. Chem.* **279,** 46981–46994 CrossRef Medline
8. Antalis, T. M., Bugge, T. H., and Wu, Q. (2011) Membrane-anchored serine proteases in health and disease. *Prog. Mol. Biol. Transl. Sci.* **99,** 1–50 CrossRef Medline
9. Antalis, T. M., Buzza, M. S., Hodge, K. M., Hooper, J. D., and Netzel-Arnett, S. (2010) The cutting edge: membrane-anchored serine protease activities in the pericellular microenvironment. *Biochem. J.* **428,** 325–346 CrossRef Medline
10. Bugge, T. H., Antalis, T. M., and Wu, Q. (2009) Type II transmembrane serine proteases. *J. Biol. Chem.* **284,** 23177–23181 CrossRef Medline
11. Netzel-Arnett, S., Hooper, J. D., Szabo, R., Madison, E. L., Quigley, J. P., Bugge, T. H., and Antalis, T. M. (2003) Membrane anchored serine proteases: a rapidly expanding group of cell surface proteolytic enzymes with potential roles in cancer. *Cancer Metastasis Rev.* **22,** 237–258 CrossRef Medline
12. Szabo, R., Wu, Q., Dickson, R. B., Netzel-Arnett, S., Antalis, T. M., and Bugge, T. H. (2003) Type II transmembrane serine proteases. *Thromb. Haemost.* **90,** 185–193 CrossRef Medline
13. Szabo, R., and Bugge, T. H. (2011) Membrane-anchored serine proteases in vertebrate cell and developmental biology. *Annu. Rev. Cell Dev. Biol.* **27,** 213–235 CrossRef Medline
14. Sales, K. U., Hobson, J. P., Wagenaar-Miller, R., Szabo, R., Rasmussen, A. L., Bey, A., Shah, M. F., Molinolo, A. A., and Bugge, T. H. (2011) Expression and genetic loss of function analysis of the HAT/DESC cluster proteases TMPRSS11A and HAT. *PLoS One* **6,** e23261 CrossRef Medline
15. Zhang, Z., Hu, Y., Yan, R., Dong, L., Jiang, Y., Zhou, Z., Liu, M., Zhou, T., Dong, N., and Wu, Q. (2017) The transmembrane serine protease HAT-like 4 is important for epidermal barrier function to prevent body fluid loss. *Sci. Rep.* **7,** 45262 CrossRef Medline
16. Sander, J. D., and Joung, J. K. (2014) CRISPR-Cas systems for editing, regulating and targeting genomes. *Nat. Biotechnol.* **32,** 347–355 CrossRef Medline
17. List, K., Haudenschild, C. C., Szabo, R., Chen, W., Wahl, S. M., Swaim, W., Engelholm, L. H., Behrendt, N., and Bugge, T. H. (2002) Matriptase/MT-SP1 is required for postnatal survival, epidermal barrier function, hair follicle development, and thymic homeostasis. *Oncogene* **21,** 3765–3779 CrossRef Medline
18. List, K., Szabo, R., Wertz, P. W., Segre, J., Haudenschild, C. C., Kim, S. Y., and Bugge, T. H. (2003) Loss of proteolytically processed filaggrin caused by epidermal deletion of matriptase/MT-SP1. *J. Cell Biol.* **163,** 901–910 CrossRef Medline
19. Madsen, D. H., Szabo, R., Molinolo, A. A., and Bugge, T. H. (2014) TMPRSS13 deficiency impairs stratum corneum formation and epidermal barrier acquisition. *Biochem. J.* **461,** 487–495 CrossRef Medline
20. Leyvraz, C., Charles, R. P., Rubera, I., Guitard, M., Rotman, S., Breiden, B., Sandhoff, K., and Hummler, E. (2005) The epidermal barrier function is dependent on the serine protease CAP1/Prss8. *J. Cell Biol.* **170,** 487–496 CrossRef Medline
21. Nagaike, K., Kawaguchi, M., Takeda, N., Fukushima, T., Sawaguchi, A., Kohama, K., Setoyama, M., and Kataoka, H. (2008) Defect of hepatocyte growth factor activator inhibitor type 1/serine protease inhibitor, Kunitz type 1 (Hai-1/Spint1) leads to ichthyosis-like condition and abnormal hair development in mice. *Am. J. Pathol.* **173,** 1464–1475 CrossRef Medline

[3] Please note that the JBC is not responsible for the long-term archiving and maintenance of this site or any other third party hosted site.

22. Szabo, R., Kosa, P., List, K., and Bugge, T. H. (2009) Loss of matriptase suppression underlies spint1 mutation-associated ichthyosis and postnatal lethality. *Am. J. Pathol.* **174,** 2015–2022 CrossRef Medline
23. Puente, X. S., Sánchez, L. M., Overall, C. M., and López-Otín, C. (2003) Human and mouse proteases: a comparative genomic approach. *Nat. Rev. Genet.* **4,** 544–558 CrossRef Medline
24. Viloria, C. G., Peinado, J. R., Astudillo, A., García-Suárez, O., González, M. V., Suárez, C., and Cal, S. (2007) Human DESC1 serine protease confers tumorigenic properties to MDCK cells and it is upregulated in tumours of different origin. *Br. J. Cancer* **97,** 201–209 CrossRef Medline
25. Updegraff, B. L., Zhou, X., Guo, Y., Padanad, M. S., Chen, P. H., Yang, C., Sudderth, J., Rodriguez-Tirado, C., Girard, L., Minna, J. D., Mishra, P., DeBerardinis, R. J., and O'Donnell, K. A. (2018) Transmembrane protease TMPRSS11B promotes lung cancer growth by enhancing lactate export and glycolytic metabolism. *Cell Rep.* **25,** 2223–2233.e6 CrossRef Medline
26. Cao, X., Tang, Z., Huang, F., Jin, Q., Zhou, X., and Shi, J. (2017) High TMPRSS11D protein expression predicts poor overall survival in non-small cell lung cancer. *Oncotarget* **8,** 12812–12819 Medline
27. Miller, G. S., Zoratti, G. L., Murray, A. S., Bergum, C., Tanabe, L. M., and List, K. (2014) HATL5: a cell surface serine protease differentially expressed in epithelial cancers. *PLoS One* **9,** e87675 CrossRef Medline
28. Ng, H. Y., Ko, J. M., Yu, V. Z., Ip, J. C., Dai, W., Cal, S., and Lung, M. L. (2016) DESC1, a novel tumor suppressor, sensitizes cells to apoptosis by downregulating the EGFR/AKT pathway in esophageal squamous cell carcinoma. *Int. J. Cancer* **138,** 2940–2951 CrossRef Medline
29. Duhaime, M. J., Page, K. O., Varela, F. A., Murray, A. S., Silverman, M. E., Zoratti, G. L., and List, K. (2016) Cell surface human airway trypsin-like protease is lost during squamous cell carcinogenesis. *J. Cell. Physiol.* **231,** 1476–1483 CrossRef Medline
30. Yueying, W., Jianbo, W., Hailin, L., Huaijing, T., Liping, G., and Shih-Hsin, L. (2008) ECRG1, a novel esophageal gene, cloned and identified from human esophagus and its inhibition effect on tumors. *Carcinogenesis* **29,** 157–160 CrossRef Medline
31. Liu, C., Li, Q., Zhou, X., Kolosov, V. P., and Perelman, J. M. (2013) Human airway trypsin-like protease induces mucin5AC hypersecretion via a protease-activated receptor 2-mediated pathway in human airway epithelial cells. *Arch. Biochem. Biophys.* **535,** 234–240 CrossRef Medline
32. Miki, M., Yasuoka, S., Tsutsumi, R., Nakamura, Y., Hajime, M., Takeuchi, Y., Miki, K., Kitada, S., and Maekura, R. (2019) Human airway trypsin-like protease enhances interleukin-8 synthesis in bronchial epithelial cells by activating protease-activated receptor 2. *Arch. Biochem. Biophys.* **664,** 167–173 CrossRef Medline
33. Menou, A., Flajolet, P., Duitman, J., Justet, A., Moog, S., Jaillet, M., Tabèze, L., Solhonne, B., Garnier, M., Mal, H., Mordant, P., Castier, Y., Cazes, A., Sallenave, J. M., Mailleux, A. A., *et al.* (2018) Human airway trypsin-like protease exerts potent, antifibrotic action in pulmonary fibrosis. *FASEB J.* **32,** 1250–1264 CrossRef Medline
34. Iwakiri, K., Ghazizadeh, M., Jin, E., Fujiwara, M., Takemura, T., Takezaki, S., Kawana, S., Yasuoka, S., and Kawanami, O. (2004) Human airway trypsin-like protease induces PAR-2-mediated IL-8 release in psoriasis vulgaris. *J. Invest. Dermatol.* **122,** 937–944 CrossRef Medline
35. Pawar, N. R., Buzza, M. S., and Antalis, T. M. (2019) Membrane-anchored serine proteases and protease-activated receptor-2–mediated signaling: co-conspirators in cancer progression. *Cancer Res.* **79,** 301–310 CrossRef Medline
36. Chokki, M., Eguchi, H., Hamamura, I., Mitsuhashi, H., and Kamimura, T. (2005) Human airway trypsin-like protease induces amphiregulin release through a mechanism involving protease-activated receptor-2-mediated ERK activation and TNFα-converting enzyme activity in airway epithelial cells. *FEBS J.* **272,** 6387–6399 CrossRef Medline
37. Orikawa, H., Kawaguchi, M., Baba, T., Yorita, K., Sakoda, S., and Kataoka, H. (2012) Activation of macrophage-stimulating protein by human airway trypsin-like protease. *FEBS Lett.* **586,** 217–221 CrossRef Medline
38. Yoshinaga, S., Nakahori, Y., and Yasuoka, S. (1998) Fibrinogenolytic activity of a novel trypsin-like enzyme found in human airway. *J. Med. Invest.* **45,** 77–86 Medline
39. Beaufort, N., Leduc, D., Eguchi, H., Mengele, K., Hellmann, D., Masegi, T., Kamimura, T., Yasuoka, S., Fend, F., Chignard, M., and Pidard, D. (2007) The human airway trypsin-like protease modulates the urokinase receptor (uPAR, CD87) structure and functions. *Am. J. Physiol. Lung Cell Mol. Physiol.* **292,** L1263–L1272 CrossRef Medline
40. Galloway, S. E., Reed, M. L., Russell, C. J., and Steinhauer, D. A. (2013) Influenza HA subtypes demonstrate divergent phenotypes for cleavage activation and pH of fusion: implications for host range and adaptation. *PLoS Pathog.* **9,** e1003151 CrossRef Medline
41. Baron, J., Tarnow, C., Mayoli-Nüssle, D., Schilling, E., Meyer, D., Hammami, M., Schwalm, F., Steinmetzer, T., Guan, Y., Garten, W., Klenk, H. D., and Böttcher-Friebertshauser, E. (2013) Matriptase, HAT, and TMPRSS2 activate the hemagglutinin of H9N2 influenza A viruses. *J. Virol.* **87,** 1811–1820 CrossRef Medline
42. Bertram, S., Heurich, A., Lavender, H., Gierer, S., Danisch, S., Perin, P., Lucas, J. M., Nelson, P. S., Pöhlmann, S., and Soilleux, E. J. (2012) Influenza and SARS-coronavirus activating proteases TMPRSS2 and HAT are expressed at multiple sites in human respiratory and gastrointestinal tracts. *PLoS One* **7,** e35876 CrossRef Medline
43. Garten, W., Braden, C., Arendt, A., Peitsch, C., Baron, J., Lu, Y., Pawletko, K., Hardes, K., Steinmetzer, T., and Böttcher-Friebertshauser, E. (2015) Influenza virus activating host proteases: identification, localization and inhibitors as potential therapeutics. *Eur J. Cell Biol.* **94,** 375–383 CrossRef Medline
44. Zmora, P., Blazejewska, P., Moldenhauer, A. S., Welsch, K., Nehlmeier, I., Wu, Q., Schneider, H., Pöhlmann, S., and Bertram, S. (2014) DESC1 and MSPL activate influenza A viruses and emerging coronaviruses for host cell entry. *J. Virol.* **88,** 12087–12097 CrossRef Medline
45. Bertram, S., Glowacka, I., Müller, M. A., Lavender, H., Gnirss, K., Nehlmeier, I., Niemeyer, D., He, Y., Simmons, G., Drosten, C., Soilleux, E. J., Jahn, O., Steffen, I., and Pöhlmann, S. (2011) Cleavage and activation of the severe acute respiratory syndrome coronavirus spike protein by human airway trypsin-like protease. *J. Virol.* **85,** 13363–13372 CrossRef Medline
46. Böttcher-Friebertshäuser, E., Freuer, C., Sielaff, F., Schmidt, S., Eickmann, M., Uhlendorff, J., Steinmetzer, T., Klenk, H. D., and Garten, W. (2010) Cleavage of influenza virus hemagglutinin by airway proteases TMPRSS2 and HAT differs in subcellular localization and susceptibility to protease inhibitors. *J. Virol.* **84,** 5605–5614 CrossRef Medline
47. Chan, R. W., Yuen, K. M., Yu, W. C., Ho, C. C., Nicholls, J. M., Peiris, J. S., and Chan, M. C. (2010) Influenza H5N1 and H1N1 virus replication and innate immune responses in bronchial epithelial cells are influenced by the state of differentiation. *PLoS One* **5,** e8713 CrossRef Medline
48. Kam, Y. W., Okumura, Y., Kido, H., Ng, L. F., Bruzzone, R., and Altmeyer, R. (2009) Cleavage of the SARS coronavirus spike glycoprotein by airway proteases enhances virus entry into human bronchial epithelial cells in vitro. *PLoS One* **4,** e7870 CrossRef Medline
49. Hsu, P. D., Scott, D. A., Weinstein, J. A., Ran, F. A., Konermann, S., Agarwala, V., Li, Y., Fine, E. J., Wu, X., Shalem, O., Cradick, T. J., Marraffini, L. A., Bao, G., and Zhang, F. (2013) DNA targeting specificity of RNA-guided Cas9 nucleases. *Nat. Biotechnol.* **31,** 827–832 CrossRef Medline
50. Cong, L., Ran, F. A., Cox, D., Lin, S., Barretto, R., Habib, N., Hsu, P. D., Wu, X., Jiang, W., Marraffini, L. A., and Zhang, F. (2013) Multiplex genome engineering using CRISPR/Cas systems. *Science* **339,** 819–823 CrossRef Medline
51. Dobin, A., Davis, C. A., Schlesinger, F., Drenkow, J., Zaleski, C., Jha, S., Batut, P., Chaisson, M., and Gingeras, T. R. (2013) STAR: ultrafast universal RNA-seq aligner. *Bioinformatics* **29,** 15–21 CrossRef Medline
52. Hartley, S. W., and Mullikin, J. C. (2015) QoRTs: a comprehensive toolset for quality control and data processing of RNA-Seq experiments. *BMC Bioinformatics* **16,** 224 CrossRef Medline
53. Love, M. I., Huber, W., and Anders, S. (2014) Moderated estimation of fold change and dispersion for RNA-seq data with DESeq2. *Genome Biol.* **15,** 550 CrossRef Medline